




Fast-tunable femtosecond visible radiation via sum-frequency generation from a high power NIR NOPO

YULIYA BINHAMMER,^{1,2,*} THOMAS BINHAMMER,³ ROBIN MEVERT,^{1,2}  TINO LANG,⁴ ANGELIKA RÜCK,⁵ AND UWE MORGNER¹

¹*Institut of Quantum Optics, Leibniz Universität Hannover, 30167 Hannover, Germany*

²*Cluster of Excellence PhoenixD (Photonics, Optics, and Engineering – Innovation Across Disciplines), 30167 Hannover, Germany*

³*NeoLase GmbH, Hollerithallee 17, D-30419 Hannover, Germany*

⁴*Deutsches Elektronen-Synchrotron DESY, Notkestrasse 85, D-22607 Hamburg, Germany*

⁵*Core Facility Confocal and Multiphoton Microscopy, University of Ulm, Ulm, Germany*

**y.binhammer@iqo.uni-hannover.de*

Abstract: We report on a high power ultra-broadband, quickly tunable non-collinear parametric oscillator with highly efficient intra-cavity sum-frequency generation. It simultaneously delivers femtosecond pulses in two synchronized output beams: up to 4.9 W tunable from 650 to 1050 nm in the near infrared and up to 1.9 W from 380 to 500 nm in the visible spectral range. The (to our knowledge) novel source is ideally suited for spectroscopy or multi-color imaging. First results of two-color functional microscopy are presented.

© 2021 Optical Society of America under the terms of the [OSA Open Access Publishing Agreement](#)

1. Introduction

With the invention of optical parametric oscillators (OPO), a tunable femtosecond light source providing a wide range of wavelengths spanning from the UV to the deep-infrared has become available [1–3]. For many years, the mainly used pump source for OPOs was the Kerr-lens mode-locked Ti:sapphire laser [4–6], which is able to deliver femtosecond pulses at high repetition rates with a few Watts of average power. Unfortunately, the well-established Ti:sapphire lasers show poor scaling potential due to the expensive green pump lasers and thermal lensing in the crystal caused by the high quantum defect. In recent years, the rapid development of high power Yb-based laser sources such as e.g. fiber amplifiers systems have opened up new scaling potential for parametric oscillators working in the near-infrared or visible spectral region. High power tunable femtosecond OPOs are of high importance for spectroscopy or imaging applications in physics, chemistry or life sciences.

Recently, we presented a non-collinear optical parametric oscillator (NOPO) [7] that delivers widely tunable femtosecond pulses from 650 nm to 1050 nm with an unprecedented tuning speed of up to 100 nm/ms as the change of operation wavelength is achieved by just varying the cavity length. Due to the non-collinear phase-matching, no adaption of crystal angle, position, or temperature is required. The fast tunability enables multi-color imaging e.g. of molecular fingerprints with orders of magnitudes faster recording speed as can be achieved by tunable Ti:sapphire lasers or tunable OPOs. While the tuning range is almost octave-spanning, the pulse spectral width and thus the spectral resolution can be tailored by setting the intracavity dispersion of the NOPO.

The wavelength tuning range of OPOs can be extended even further by an additional nonlinear conversion stage. In contrast to passively mode-locked laser oscillators, even intra-cavity processes are supported with high efficiency. This has been successfully demonstrated by several

groups for the case of intra-cavity second harmonic or sum-frequency generation for OPOs based on periodically poled crystals [8–11]. However, all these studies rely on narrowband phase-matching and thus suffer from slow tuning speed.

In this work, we combine the ultra-broad bandwidth and fast tunability of the NOPO with an intra-cavity SFG process of similar phase-matching bandwidth. This way, the ultrafast tuning capabilities are preserved while adding a second output channel ranging from 390 nm to 520nm. Thus, a novel unique femtosecond light source with two synchronized output pulse trains covering almost the full visible and near-infrared wavelength regime is presented, which is ideally suited for femtosecond spectroscopy and fast multi-color imaging techniques like excitation fingerprinting or hyperspectral microscopy.

2. Experimental setup

The schematic setup of the NIR NOPO, designed as a singly resonant ring cavity with a second focus for sum-frequency generation, is shown in Fig. 1. A 2.2 mm long BBO crystal, cut for type I phase matching ($\theta = 24.65^\circ$), is used as gain medium. In order to achieve a simultaneous broadband phase-matching a non-collinear geometry with an angle between pump and signal beam is required. Due to the birefringence of BBO, there are two non-equivalent configurations [12]: For the so-called Poynting vector walk-off compensation geometry (PVWC), the ordinarily polarized signal beam is incident at a – per definition – positive non-collinear angle and its \mathbf{k} vector is pointing in the direction of the Poynting vector \mathbf{S} of the extra-ordinarily polarized pump. This geometry therefore shows reduced effects from a walk-off between signal and pump pulses during propagation. The opposite orientation with a negative angle between signal and pump beam is called tangential phase-matching geometry (TPM). Here, the \mathbf{k} vector of the signal

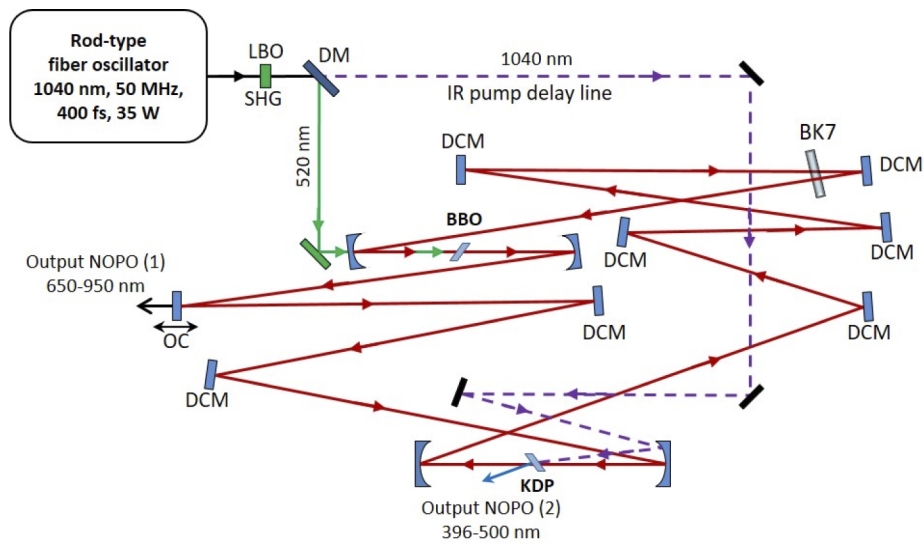


Fig. 1. Schematic setup of the 2-foci NIR NOPO with intracavity sum-frequency generation. LBO: SHG crystal (2.5 mm), DM: dichroic mirror (HR 515, AR 1030), BBO: nonlinear crystal (2.2 mm), DCM: double-chirped mirror pairs, KDP: nonlinear crystal SFG (1.5 mm), BK7: AR-coated N-BK7 broadband window (12 mm), OC: output coupler 660 -920 nm (various output coupling ratios have been used in the range of 0.2% to 25%). The total resonator length is corresponding to the fiber oscillator repetition rate of 50 MHz and the separation of the curved mirrors (all with a radius of curvature of 100 mm) is approx. 103 mm.

beam points away from the Poynting vector of the pump and therefore stronger effects from walk-off are observed. For the small pump focal radius of less than 20 μm used in the NOPO, the PVWC geometry is favorable [13] and has been chosen with an angle of 2.4° between the pump beam and resonator beam for the ultrabroadband phase-matching ranging from 650 to 1050 nm. All intra-cavity mirrors, plane and curved (100 mm radius of curvature in both foci) are double-chirped mirror pairs (DCM) supporting a spectral range of 600-1200 nm [14]. The NOPO is synchronously pumped by the second harmonic of a home-built rod-type fiber MOPA offering up to 35 W of output power at 1040 nm with 400 fs pulses at 50 MHz repetition rate. The second harmonic pump radiation is generated in a 2.5 mm LBO crystal with up to 23 W of average power. It is focused into the gain crystal by a 150 mm focusing lens through one of the folding mirrors, which offer a transmission of more than 95% in a spectral window from 510nm to 540nm for the pump. The remaining IR pulses from the frequency-doubling stage are then separated from the green pump with a dichroic mirror (DM) and are re-used as pump for the sum-frequency process in the second focus. The details of the SFG process will follow in section 3.2. As described in [7] in more detail, a net positive intra-cavity dispersion is required to establish a stable operation of the NOPO. The parametric gain initially supports a broadband signal pulse which is stretched further with each roundtrip by the intra-cavity dispersion until it is eventually spectrally filtered in the time domain by the short pump pulse. The chirp therefore can be used to control the spectral bandwidth of the NOPO pulses. In our setup, the positive intracavity dispersion is provided by an intra-cavity 12 mm BK7 plate in double pass.

3. Experimental results

3.1. High power ring cavity NIR NOPO

At first, we explored the scaling potential of the NIR NOPO using up to 20 W of the second harmonic pump. At this power level, the peak intensity at the crystal already reaches a level exceeding 100 GW/cm^2 . Further increase of the pump power leads to higher-order nonlinear effects such as white light generation, plasma formation, and eventually to the destruction of the crystal. Nevertheless, further power scaling of the NOPO is intrinsically possible by adapting the focusing geometries of the resonator and the pump.

With an output coupling ratio of 25%, we achieve a slope efficiency of approx. 30% and more than 5 W of average power in collinear alignment, which only allows narrowband operation. This high power level can be maintained by changing to the non-collinear PVWC geometry required for broadband operation as presented in Fig. 2(a). The comparison between a pump power of 8 W and 18 W shows that the power over the entire spectral range from 650 to 1050 nm is increased with a slightly larger tuning range at higher powers. There is a pronounced drop in output power around 920 nm which is caused by parasitic second-harmonic phase matching in the PVWC geometry. However, the NOPO still delivers more than 1 W of output power in this region.

In Fig. 2(b), a few selected spectra for different center wavelengths are depicted exemplarily. As no adaption of the crystal angle or intra-cavity re-alignment is required, the NOPO allows for a tuning mechanism by varying the cavity length only [15], and thus uniquely fast tuning speeds $>100 \text{ nm/ms}$ are achieved. The NOPO spectra have a transform limit in the range of 100 fs, with an increase of spectral bandwidth towards the near IR end of the tuning range, which can be attributed to the intra-cavity third-order dispersion leading to lower positive chirp at longer wavelengths. This nicely illustrates that the bandwidth of the NOPO pulses can be easily adjusted by setting the intra-cavity chirp, as long as it is sufficiently high to guarantee stable pulse formation [7].

Especially in case of two-photon imaging, the spectral region from 900 nm to 950 nm is of high importance and the reduced output power as well as the slightly broadened spectrum of the NOPO in this region are unfavorable for this application. The parasitic second harmonic generation causing this effect is the major drawback of the PVWC geometry and is not present

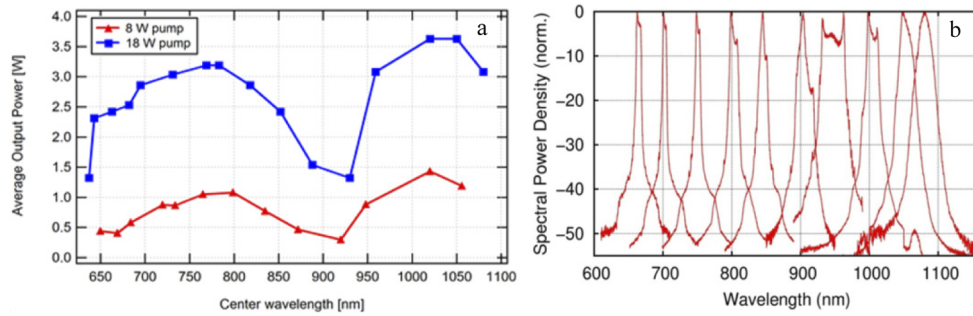


Fig. 2. a: Scaling properties of the IR NOPO showing the average output power of the parametric oscillator in non-collinear geometry for two different pump powers. b: Selected signal spectra.

for the tangential phase matching. Based on our previous work [13], however strong walk-off effects for TPM geometry with the given pump focus and crystal length are expected, so it is not clear, if the NOPO operation is possible. As a proof of principle, this was tested by changing the pump and signal alignment to the tangential geometry. A broadband operation from 800 nm to 1000 nm can also be achieved in this configuration with more than 3 W of output power and an almost Gaussian spectral tuning profile. For the presented setup with a pump focal radius of less than 20 μm , we observed high signal beam displacement in the cavity while tuning and a less broadband tuning range in comparison to the results achieved in PVWC geometry. It can be concluded, that the operation of the NOPO in TPM geometry is possible with a smooth tuning in the spectral region around 900 nm, but a larger pump spot size and a shorter BBO crystal would be required to reduce walk-off effects. As the goal of this work was focused on the most broadband operation, all presented results were obtained in PVWC geometry.

3.2. Intra-cavity sum-frequency generation in a NIR NOPO

As discussed above, the NOPO concept offers a wide tuning range and scaling properties superior to current state-of-the-art Ti:sapphire based laser systems. An additional advantage is the potential for intra-cavity wavelength conversion. In ultrafast laser oscillators, the mode-locking mechanism relies on saturable absorbers as for example the Kerr lens mechanism. This absorber supports the formation of short and intense pulses over the continuous operation, as the cavity losses decrease with pulse intensity. Intra-cavity nonlinear frequency conversion as SHG, SFG, or DFG however counteracts the mode-locking mechanism, as higher pulse intensities lead to higher conversion and thus increased losses for the fundamental pulse. Therefore, this concept is limited to low efficiency in case of traditional mode-locked oscillators.

Pulse formation in a synchronously pumped NOPO is established in a completely different way. A broadband high gain is provided by the parametric process and the initiated super-fluorescence is traveling through the ring cavity which shows a positive dispersion. After one roundtrip, only these spectral components are actively seeded into the parametric amplification process that arrive in temporal overlap with the pump pulse. In simple terms, mode-locking is established as an interplay of temporal filtering and positive dispersion. Introducing an efficient nonlinear conversion stage is therefore possible, as long as the parametric gain supersedes the nonlinear losses for a given wavelength. This allows conversion efficiencies on the order of 20% [16] and offers an even wider spectral operation range for the NOPO by implementing a nonlinear conversion stage in the second intra-cavity focus.

As one of the most imminent applications for the NOPO is spectroscopy and imaging [17,18], we chose a conversion to the visible spectral region. This can be achieved by sum frequency

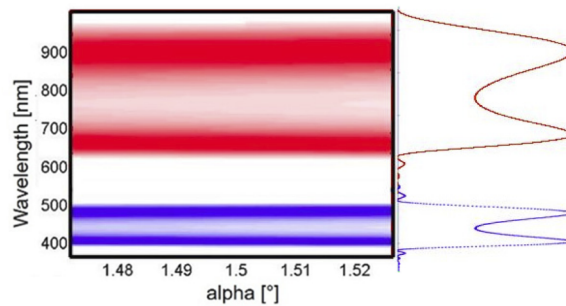


Fig. 3. Phase-matching in the KDP crystal cut at $\theta=56^\circ$ for type II SFG. Pump: 1040 nm; Signal (red) 650 nm to 950 nm; resulting VIS radiation tunable from 400 to 500 nm (blue) with a non-collinear angle α between signal and pump around 1.5° . The color shading indicates the normalized conversion efficiency scaled from 0 to 1 as depicted by the line out on the right.

generation of the intra-cavity signal pulses with the remaining fundamental pump light behind the frequency doubling stage (see Fig. 1) which is intrinsically synchronous to the NOPO pulses. In order to maintain the intrinsic fast tunability of the NOPO over the entire spectral range, a broadband phase matching of the sum-frequency conversion is required. In our case, it has been realized in a 1.5 mm thin KDP crystal with focal radius of 18 μm for the intra-cavity beam. Figure 3 demonstrates the broadband non-collinear SFG phase-matching in the KDP crystal (cut at $\theta=56^\circ$; type II ($o+e\rightarrow e$)), where the ordinarily polarized intra-cavity pulses in the range of 650-950 nm (red) are mixed with the extraordinarily polarized IR pump to generate extraordinary polarized sum-frequency (blue). This process with a non-collinear angle of $\alpha = 1.5^\circ$ allows targeting a visible spectral region from 390 nm to 520 nm without the need of changing the crystal angle while tuning. The non-collinear configuration for SFG allows overlapping the IR pump with the cavity beam in the KDP crystal as well as the extraction of the generated blue from the cavity (see Fig. 1) without the requirement of a special transmission window in the coating of the curved folding mirrors.

The measured tuning properties of the NOPO with intra-cavity SFG are presented in Fig. 4. The NOPO is operated at a pump power of 9.1 W with a 1% output coupler. The VIS output is re-collimated with an $f = 50$ mm fused silica lens. By tuning the NOPO, the VIS output follows from 402 nm to 500 nm. With 4.3 W of power in the residual 1040 nm beam, up to 900 mW could be extracted at 420 nm (blue curve); the NIR output behind the 1% OC exceeds 100 mW over the whole tuning range (red curve). In the presented configuration with 1% of IR output coupling, at the maximum visible output of 900 mW at 420 nm, the IR output provides 500 mW at 720 nm. On the first glance, a higher efficiency could be expected as the intra-cavity power within the NOPO is approximately 40 W. However, the spatial and temporal overlap is very important for a good conversion. The auxiliary IR beam used in our case is strongly distorted in both aspects as it is the left-over from an efficient SHG generation stage. This limits the SFG power conversion efficiency to about 20% in respect to the incident auxiliary IR pulse. An easy way to avoid this issue would be a separation of an auxiliary pulse from the IR pump before second harmonic generation. With a better and stronger IR beam, much higher extraction efficiency of the VIS radiation is definitely feasible.

The spectral width of the VIS pulses is following the NIR spectra and can be influenced and adapted the same way by the internal dispersion settings. The VIS pulses show a typical bandwidth supporting sub-100 fs pulses, but the measured autocorrelation yields a longer pulse duration. Assuming a deconvolution factor of 0.707 for a Gaussian pulse shape, a pulse duration of 290 fs is obtained at 448 nm as shown exemplarily in Fig. 5 (left) and a slightly shorter pulse

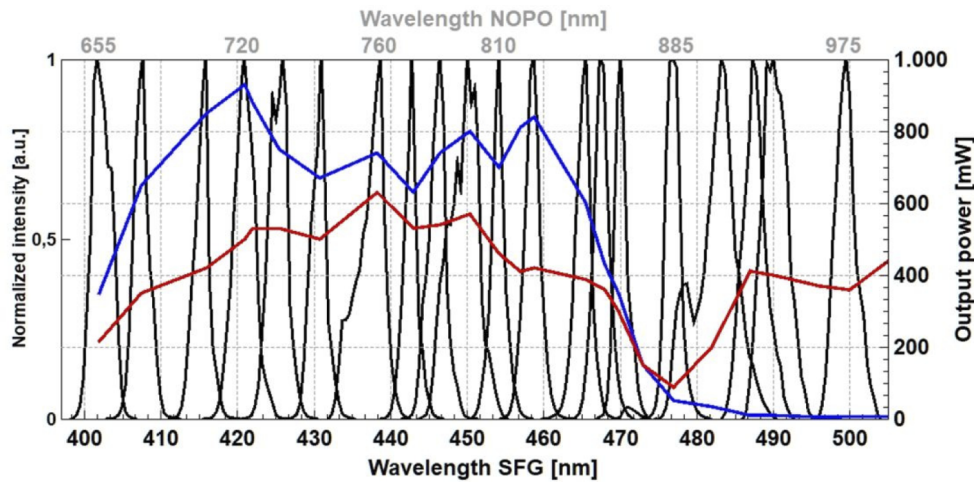


Fig. 4. Tuning behavior of the SFG pulses generated by nonlinear output coupling from the NOPO. Some normalized SFG spectra are plotted (left axis) with the corresponding output power (blue curve, right axis). The top labels show the corresponding NOPO center wavelengths; the respective NOPO output powers follow the red curve.

duration is measured for longer wavelength e.g. 205 fs at a center wavelength of 474 nm. As the signal pulses in the NOPO are positively chirped due to the net positive cavity dispersion, it can be assumed, that this chirp is also transferred to the pulses generated by SFG in the VIS, which explains the discrepancy between transform-limit and measured pulse duration.

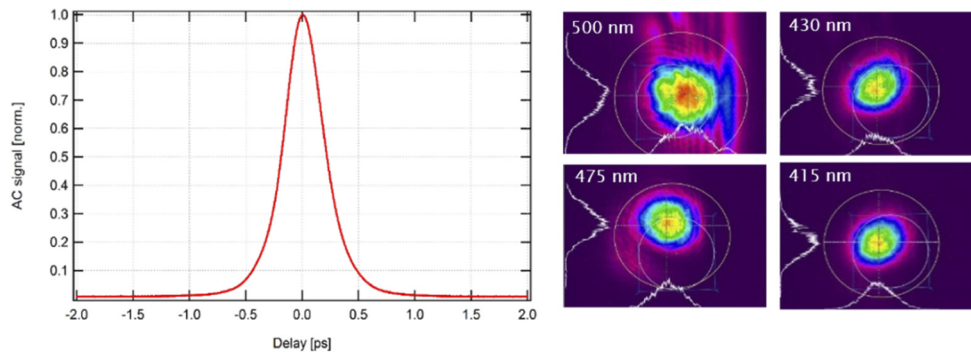


Fig. 5. Left: Measured autocorrelation trace of the SFG signal at 470 nm corresponding to a pulse duration of 300 fs. Right: Beam profiles of the generated SFG pulses for different wavelengths.

Important aspect for any application is the beam profile and pointing associated with the wavelength tuning in the visible. As it is generated by a non-collinear SFG process, some walk-off can be expected here. By a simple k -vector momentum conservation argument, a theoretical angle deviation between the emission of SFG at the spectral edges at 390 nm and 520 nm amounts to 3.5 mrad. With the short re-collimation distance of 50 mm, this would lead to a beam displacement of less than 200 μm of the SFG output beam. In Fig. 5 (right) the beam profiles at approx. 1 m distance behind the re-collimation lens are shown. The profile remains Gaussian over the full tuning range, and the center position is moving less than 500 μm on the camera, which is

in qualitative agreement with the theoretical expectation. In practice, this will not impose any severe limitation in spectroscopy or imaging applications.

The power and wavelength stability of the free-running NOPO strongly depends on the lab conditions, as it is affected by the respective frequency drift of two resonators, namely the used fiber seed oscillator and the NOPO cavity. As the cavity length can be used to tune the spectrum, the center wavelength of the NOPO will also change in reverse, when the NOPO cavity length is drifting against the fiber seed oscillator. After a warm-up time of 10 min, a spectral drift of approximately 2 nm/min was observed and the output power exhibited a noise of 1.5% rms over 30 min for the NIR output and 2.7% for the SFG. Both properties can be drastically improved by implementing an active stabilization of the pump beam position and angle (Aligna, TEM Messtechnik) as well as the NOPO cavity length (see section 3.4). This allowed an operation of the NOPO with a stability of the center wavelength of less than 0.5 nm and a power stability of the NIR output < 2% rms over a period of 8 hours.

3.3. Versatility of system parameters

As presented above, the concept of broadband non-collinear phase matching for both fundamental NOPO signal pulses and the SFG pulses in the VIS allows for fast tunability with two synchronous femtosecond pulse train outputs in the IR and VIS region separated by a constant frequency offset of 290 THz. The scaling potential of the NOPO discussed in section 3.1 was also demonstrated together with the VIS conversion. The power ratio between the two output branches can be varied by changing the output coupler transmission. An overview of the achievable output power at an exemplarily chosen wavelength of 450 nm for the VIS (in blue) and 793 nm for the IR output (in red) is given in Fig. 6. With a 15% output coupler, more than 3.6 W were achieved in the IR at 22 W pump power with a corresponding VIS output of more than 1.1 W. For a “closed” NOPO cavity, i.e. using a high reflecting mirror instead of an output coupler, more than 1.9 W from the SFG is achieved. The high intra-cavity power however destabilizes the system due to heating up of components by the generated idler photons, which are emitted under an angle with an estimated average power of several Watts.

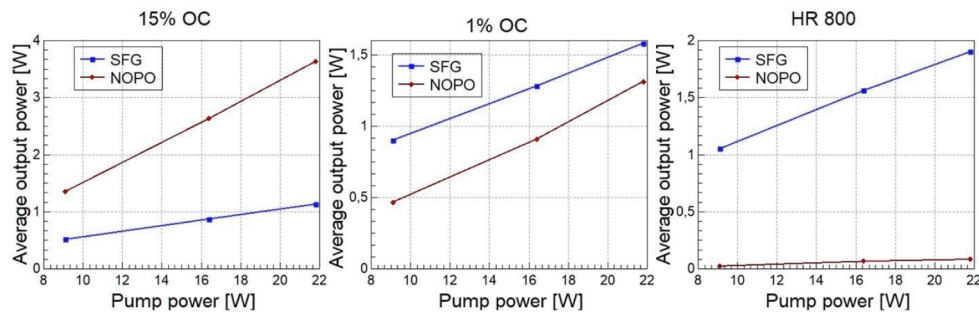


Fig. 6. Scaling of the NOPO NIR output power (red line) and the respective intracavity SFG power (blue line) for three different output coupler transmission values, namely 15% (left), 1% (middle) and a high reflecting mirror with a reflectivity of 99.8% used as an output coupler with respective transmission of 0.2% (right).

The presented scheme of OPO intra-cavity frequency conversion is quite versatile and opens up new directions. A DFG process in the second crystal could be used to reach the MID-IR region; furthermore, an auxiliary beam at the second harmonic of the pump laser can be employed to reach other spectral regions. The system maintains its ultrafast tuning capabilities as long as a broadband phase matching for the conversion process can be found. It should also be mentioned

that in addition to the NOPO output, a strong idler pulse is generated, which is currently not used as it is emitted at a spectrally varying angle (which could be, however, compensated [19]).

3.4. Application: Ultrafast multi-color imaging

With the demonstrated tunability range, the NOPO is ideally suited to specifically address a wide range of fluorophores used in two-photon microscopy. Moreover, the ultrafast tuning speed allows for orders of magnitude higher imaging rates than with traditionally used tunable Ti:sapphire lasers. For the two-photon imaging experiments, only the IR output of the NOPO was used. For fast tuning, it was equipped with a piezo-actuated folding mirror to control and select the excitation wavelength as well as a fast CCD spectrometer (TEM Messtechnik). An additional slow motorized end mirror was implemented to compensate for long-term drifts between the pump oscillator and the NOPO cavity length. These modifications allowed for stable operation of the NOPO with reproducible wavelength addressing for several hours. As a first demonstration of the NOPO capabilities, two-photon images of cells, stained with three colors and excited with two wavelengths of the NOPO (at 750 and 840 nm) in a modified Zeiss microscope (LSM 7MP) have been recorded. In Fig. 7, a multi-color IEC6 cell system is shown, which has been incubated with the fluorescent dyes DAPI (4,6-Diamidino-phenylindol), Alexa 430 tubulin and mitotracker red. For DAPI, an excitation wavelength of 750 nm has been chosen, whereas mitotracker red was excited at 840 nm. Alexa 430 tubulin was excited with both wavelengths. The NOPO was set-up to switch between these two wavelengths as quickly as possible, staying on the line during the detection and switching back again.

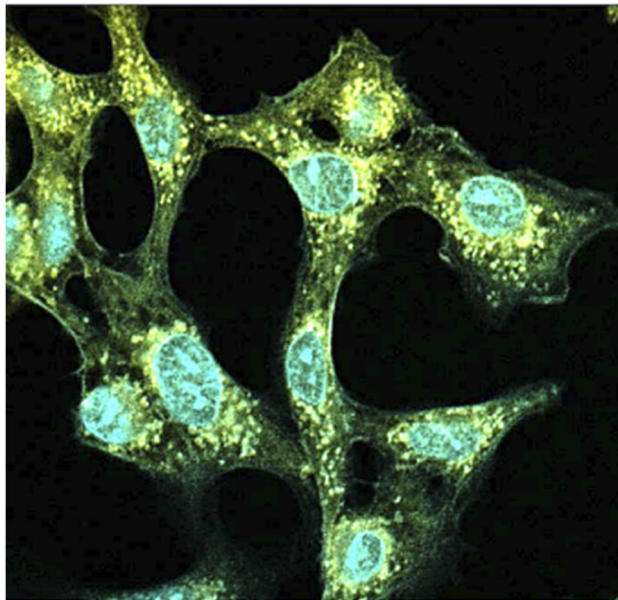


Fig. 7. Multi-color IEC6 cell system of three colors, excited with a two wavelength multi-track excitation mode. The IEC6 cells were incubated with DAPI (shown in blue color), Alexa 430 Tubulin (in green color), Mitotracker red (in yellow color). Multi-track by excitation of DAPI (750 nm) and Mitotracker Red (840 nm). Alexa 430 was excited by both wavelengths. The total recording time was three seconds.

The change between those two wavelengths could be done in less than 1 ms, which allowed a line-by-line detection of the two different fluorophores. The total recording time of the sample was only 3 seconds, compared to approximately 5 min by using a conventional Ti:sapphire

laser in the similar conditions with the same sample. Please note that the switching speed was only technically limited and can be, in principle, increased to > 500 nm/ms [20] by using e.g. electro-optical switching. This would allow a pixel-by-pixel change of color and therefore a quasi-instantaneous multi-color imaging of the sample. It also paves the way to specifically separate multiple fluorophores in complex cell structures by excitation fingerprinting instead of normally used emission fingerprinting. Another related example of a possible application of the NOPO is the determination of the ratio and oxidation status of NADH and FAD, natural fluorophores in biological tissues that can be used as a metabolic indicator to detect tumor. In this case, different excitation wavelengths are required to clearly separate NADH and FAD, due to their emission/excitation spectra overlap [21,22].

4. Conclusion and outlook

We presented the implementation of intra-cavity nonlinear output coupling within a non-collinear OPO, extending the unique ultra-wide and rapid tuneability to the visible wavelength range. In contrast to Ti:sapphire lasers, intra-cavity processes can be driven in an optical parametric oscillator with high conversion rates due to the high intra-cavity gain and the stable pulse formation mechanism. The scaling capabilities of the NOPO concept pumped by an Yb-based femtosecond amplifier system is shown for the comparison of two different pump powers, namely 8W and 18W, and we strongly believe, the average power of the NOPO can be further scaled to higher pump powers by increasing the pump spot size and adapting the radius of curvature of the cavity focussing mirrors accordingly. We presented the implementation of intra-cavity sum-frequency generation into a second output beam in the visible spectral range. The process is phase-matched over a broad bandwidth, thereby maintaining the unique ultrafast tuning properties of the NOPO concept. The novel light source simultaneously delivers high power femtosecond pulses in the near infrared and visible spectral range and is thus ideally suited for spectroscopy or multi-color imaging in life sciences. A first demonstration of the potential of the NOPO is shown for the case of two-photon microscopy of a multi-color IEC6 cell system. Here, the ultrafast tuning speed enables multi-color imaging with much faster image acquisition of just 3 sec compared to the 5 minutes performed with a conventional Ti:sapphire source. The time required for switching is limited by mechanics only. Whereas the complexity of the NOPO might be still an obstacle for clinical usage, it is comparable to Ti:sapphire lasers which are widely used in bioscience laboratories. The presented concept of an intra-cavity nonlinear output coupling by sum-frequency generation is power scalable and could be applied also to other nonlinear processes. For example, difference frequency generation can extend the wavelength range to the MID-IR spectral region- The NOPO with intra-cavity sum-frequency generation is thus a versatile source for different imaging techniques, for example: CARS, Raman spectroscopy, FLIM, etc.

Funding. Germany's Excellence Strategy within the Cluster of Excellence PhoenixD (390833453, EXC 2122); Bundesministerium für Bildung und Forschung (13N12940).

Acknowledgement. The authors thank our cooperation partners Carl Zeiss Microscopy GmbH, Laser Quantum Ltd and TEM Messtechnik for their support. This work was funded by the Bundesministerium für Bildung und Forschung (BMBF) within the METAPHOR project (13N12940) and by Germany's Excellence Strategy within the Cluster of Excellence PhoenixD (EXC 2122, Project ID 390833453).

Disclosures. The authors declare that there are no conflicts of interest related to this article.

Data availability. Data underlying the results presented in this paper are not publicly available at this time but may be obtained from the authors upon reasonable request.

References

1. M. Ebrahim-Zadeh, "Optical parametric oscillators: New breakthroughs in mid-infrared," in *Optics InfoBase Conference Papers* (OSA, 2019), Part F134-, p. NTu3B.1.

2. M. Ebrahim-Zadeh, "New frontiers in optical parametric oscillators," in *Optics InfoBase Conference Papers (OSA, 2018)*, Part F123-, p. Tu3B.1.
3. C. F. O'Donnell, S. Chaitanya Kumar, P. G. Schunemann, and M. Ebrahim-Zadeh, "Femtosecond optical parametric oscillator continuously tunable across 36–8 μm based on orientation-patterned gallium phosphide," *Opt. Lett.* **44**(18), 4570 (2019).
4. D. E. Spence, S. Wielandy, C. L. Tang, C. Bosshard, and P. Günter, "High-repetition-rate femtosecond optical parametric oscillator based on KNbO₃," *Opt. Lett.* **20**(7), 680 (1995).
5. G. M. Gale, M. Cavallari, and F. Hache, "Femtosecond visible optical parametric oscillator," *J. Opt. Soc. Am. B* **15**(2), 702 (1998).
6. M. Ghotbi, A. Esteban-Martin, and M. Ebrahim-Zadeh, "BiB 3 O 6 femtosecond optical parametric oscillator," *Opt. Lett.* **31**(21), 3128 (2006).
7. T. Lang, T. Binhammer, S. Rausch, G. Palmer, M. Emons, M. Schultze, A. Harth, and U. Morgner, "High power ultra-widely tuneable femtosecond pulses from a non-collinear optical parametric oscillator (NOPO)," *Opt. Express* **20**(2), 912 (2012).
8. A. Esteban-Martin, O. Kokabee, and M. Ebrahim-Zadeh, "Efficient, high-repetition-rate, femtosecond optical parametric oscillator tunable in the red," *Opt. Lett.* **33**(22), 2650–2652 (2008).
9. T.-Y. Jeong, S.-H. Kim, G.-H. Kim, and K.-J. Yee, "Visible-pulse generation in gain crystal of near-infrared femtosecond optical parametric oscillator," *Opt. Express* **23**(20), 25620–7 (2015).
10. C. Gu, M. Hu, L. Zhang, J. Fan, Y. Song, C. Wang, and D. T. Reid, "High average power, widely tunable femtosecond laser source from red to mid-infrared based on an Yb-fiber-laser-pumped optical parametric oscillator," *Opt. Lett.* **38**(11), 1820 (2013).
11. K. Devi, S. Chaitanya Kumar, and M. Ebrahim-Zadeh, "Fiber-laser-based, high-repetition-rate, picosecond ultraviolet source tunable across 329–348 nm," *Opt. Lett.* **41**(20), 4799 (2016).
12. J. Bromage, J. Rothhardt, S. Hädrich, C. Dorrer, C. Joher, S. Demmler, J. Limpert, A. Tünnermann, and J. D. Zuegel, "Analysis and suppression of parasitic processes in noncollinear optical parametric amplifiers," *Opt. Express* **19**(18), 16797–808 (2011).
13. T. Lang, A. Harth, J. Matyschok, T. Binhammer, M. Schultze, and U. Morgner, "Impact of temporal, spatial and cascaded effects on the pulse formation in ultra-broadband parametric amplifiers," *Opt. Express* **21**(1), 949 (2013).
14. F. X. Kärtner, U. Morgner, R. Ell, T. Schibli, J. G. Fujimoto, E. P. Ippen, V. Scheuer, G. Angelow, and T. Tschudi, "Ultrabroadband double-chirped mirror pairs for generation of octave spectra," *J. Opt. Soc. Am. B* **18**(6), 882 (2001).
15. T. Lang, T. Binhammer, S. Rausch, G. Palmer, M. Emons, M. Schultze, A. Harth, and U. Morgner, "Rapidly spectral ramping of an ultra-wide tuneable femtosecond non-collinear optical parametric oscillator with high average output power," in *Advanced Solid-State Photonics, ASSP 2012* (Optical Society of America (OSA), 2012), p. AT2A.2.
16. M. Ghotbi, A. Esteban-Martin, and M. Ebrahim-Zadeh, "Tunable, high-repetition-rate, femtosecond pulse generation in the ultraviolet," *Opt. Lett.* **33**(4), 345–347 (2008).
17. L. Beichert, Y. Binhammer, J. R. Andrade, A. K. Kniggendorf, B. Roth, and U. Morgner, "Non-collinear optical parametric oscillator for video rate stimulated raman spectroscopy of microplastics," in *2019 Conference on Lasers and Electro-Optics Europe and European Quantum Electronics Conference* (Optical Society of America, 2019), (2019), p. paper cd_2_5.
18. L. Beichert, Y. Binhammer, J. R. Andrade, A. K. Kniggendorf, B. Roth, and U. Morgner, "Non-collinear Optical Parametric Oscillator as fast tuneable light source for Stimulated Raman Scattering," in *9th EPS-QEOD Europhoton Conference, (Online Conference)* (2020).
19. M. Mero and V. Petrov, "High-Power, Few-Cycle, Angular Dispersion Compensated Mid-Infrared Pulses from a Noncollinear Optical Parametric Amplifier," *IEEE Photonics J.* **9**(3), 1–8 (2017).
20. A. Pape, T. Binhammer, Y. Khanukaeva, T. Lang, J. Ahrens, O. Prochnow, and U. Morgner, "Ultrafast spectral switching of a Non-collinear Optical Parametric Oscillator (NOPO)," in *International Conference on Ultrafast Phenomena* (Optical Society of America, 2016), p. UW4A.43.
21. S. Kalinina, J. Breymayer, K. Reeß, L. Lilge, A. Mandel, and A. Rück, "Correlation of intracellular oxygen and cell metabolism by simultaneous PLIM of phosphorescent TLD1433 and FLIM of NAD(P)H," *J. Biophotonics* **11**(10), e201800085 (2018).
22. A. Rück, P. Schäfer, B. von Einem, I. S. Kritchenkov, and S. Kalinina, "Metabolic NADH/FAD/FMN FLIM and oxygen PLIM: multiphoton luminescence lifetime imaging on the way to clinical diagnosis," in *Multiphoton Microscopy in the Biomedical Sciences XX*, A. Periasamy, P. T. C. So, and K. König, eds. (SPIE, 2020), 11244, pp. 6–13.